Weddell Sea Polynya analysis using SMOS-SMAP Sea Ice Thickness Retrieval

Alexander Mchedlishvili[1], Gunnar Spreen[1], Christian Melsheimer[1], and Marcus Huntemann[1]

[1]University of Bremen, Institute of Environmental Physics, Bremen, Germany

Correspondence: Alexander Mchedlishvili (alexander.mchedlishvili@uni-bremen.de)

Abstract.

The Weddell Sea Polynya is an anomalous large opening in the Antarctic sea ice above the Maud Rise seamount. After 40 years of absence, it fully opened again on 13 September, 2017, and lasted until melt; staying open for a total of 80 days. 2017, however, actually was not the only year the imprint of the polynya could be identified. By investigating sea ice thickness (SIT) data retrieved from the satellite microwave sensors Soil Moisture Ocean Salinity (SMOS) and Soil Moisture Active Passive (SMAP), we have isolated an anomaly of thin sea ice spanning an area comparable to the polynya of 2017 over Maud Rise occurring in September 2018. In this paper, we look at sea ice above Maud Rise in August and September of 2017 and 2018 as well as all years from 2010 until 2020 in a 11-year time series. Using the ERA5 surface wind reanalysis data, we present the strong impact storm activity has on sea ice and help consolidate the theory that the Weddell Sea Polynya, in addition to oceanographic effects, is subject to direct atmospheric forcing. Based on the results presented we propose that the Weddell Sea Polynya, rather than being a binary system with one principal cause, is a dynamic process caused by various different preconditioning factors that must occur simultaneously for it to occur. Moreover, we show that rather than an abrupt stop to anomalous activity atop Maud Rise in 2017, the very next year shows signs of polynya-favourable activity that, although insufficient, was present in the region. This effect, as will be shown in the 11-year SMOS record, is not unique to 2018 and similar anomalies are identified in 2010, 2013 and 2014. It is demonstrated that L-band microwave radiometry from the SMOS and SMAP satellites can provide additional useful information, which helps to better understand dynamic sea ice processes like polynya events, in comparison to if satellite sea ice concentration products would be used alone.

1 Introduction

From 1974 to 1976, for three consecutive winters, the satellite microwave radiometer record shows a roughly $250 \cdot 10^3$ km^2 opening in sea ice near the Maud Rise seamount (Cheon and Gordon, 2019). For the next 40 years no sizeable opening in sea ice is documented except for an occasional low sea ice concentration (SIC) halo around Maud Rise (Lindsay et al., 2004). Only in 2016 and more so in 2017 is anything comparable to the polynya of 1974 to 1976 detected again. For the purposes of this paper, we will define both the 1970s and 2010s occurrences as the Weddell Sea Polynya despite their differences.

The Weddell Sea Polynya is an anomalous opening in sea ice that is generally classified as an open-ocean polynya (e.g., Cheon and Gordon, 2019; Campbell et al., 2019; Jena et al., 2019). An open-ocean or 'sensible heat' polynya is distinguished

from the coastal 'latent heat' polynya by being maintained and opened by upwelling of above freezing temperature water from below as opposed to wind-driven ice advection. Cheon and Gordon (2019) describe this process in detail by explaining the preconditioning as well as the eventual closing of the polynya. They attribute the polynya to the weakening of the upper ocean stratification which leads to a destabilization of the water column and thereby convection. The newly formed convection

30 cell pushes up Warm Deep Water which melts the overlying sea ice and stops the surface water layer from refreezing. Cheon and Gordon (2019) admit to atmospheric influences, specifically the influence of positive Southern Annular Mode (SAM) which intensifies the negative wind stress curl over the Weddell Sea and thereby the Weddell Gyre, but do not discuss direct atmospheric effects in detail, which we explain later. Campbell et al. (2019) confirm previously mentioned oceanographic influence and also present proof of how intense storm events occurring locally near Maud Rise aid the formation of the

35 polynya. Storm activity characterised by strong winds contributes to ice divergence and enhanced turbulent mixing (Campbell et al., 2019). Ice divergence due to strong winds enables rapid ice production and brine rejection as with coastal polynyas. In the case of the Weddell Sea Polynya this process prevents immediate stabilization from ice melt as wind-driven turbulent mixing entrains heat and salt into the surface mixed layer, a response that is amplified under weak stratification.

Last but not least it is important to discuss why this occurs specifically at Maud Rise as thus far all discussed preconditioning

40 is by no means exclusive to the sea ice within the region of interest. In the region of Maud Rise, anomalously warm waters are found over the flanks of the rise, with a colder cap of water lying over the top of the rise (e.g., Lindsay et al., 2004; Muench et al., 2001; Bersch et al., 1992). Muench et al. (2001) go further to state that Maud Rise facilitates an upward transport of Warm Deep Water forming an ocean region characterised by its upper ocean heat flux that is roughly twice the size of the topographic formation itself. This anomalous body of water is partially isolated from surrounding water masses by virtue of

45 the Taylor column that is caused by the Coriolis effect. Rotating fluids, in this case the Antarctic Circumpolar Current, that are perturbed by virtue of the underlying topographic obstruction (Maud Rise) tend to form columns parallel to the axis of rotation called Taylor columns; these columns end up becoming isolated from surrounding waters thereby further facilitating the formation of convection cells in the region. Due to the presence of Maud Rise and the surrounding elevated Warm Deep Water, the 23–year local mean Sea Ice Concentration (SIC) for the months of July through November (1979–2001) shows a

50 distinctive nearly-circular halo of low ice concentration with a diameter of about 300 km (Lindsay et al., 2004) but lacks the open water expanse indicative of a polynya.

In part, this study aims to contribute to the recently-emerging understanding of direct atmospheric influence over the Maud Rise region and support the notion that the Weddell Sea Polynya is not purely an ocean-driven polynya (Heuzé and Lemos, in review, 2020). However, the primary investigation is done during polynya-free years. Through analysis of the sea ice thickness

55 (SIT) product from the spaceborne passive microwave sensors Soil Moisture Ocean Salinity (SMOS) and Soil Moisture Active Passive (SMAP) in the combined SMOS-SMAP SIT retrieval, we aim to reverse the notion that anomalous activity atop Maud Rise is purely a binary system. Rather, the Weddell Sea Polynya is the result of independent as well as dependent preconditioning effects that occasionally but not exclusively interfere with one another constructively to form the polynya, like in 2016, 2017 and mid-1970s. Using the SIT retrieval over years where the polynya did not occur, we aim to identify low sea

60 ice thicknesses that demonstrate anomalous behaviour taking place in the absence of the Weddell Sea Polynya suggesting the

existence of polynya-favorable conditions that although present are insufficient to produce the polynya. Previous studies use satellite sea ice concentration to analyse the size and development of the polynya. Since 2010, the SMOS satellite has allowed us to analyse thin ice area anomalies, i.e., thinning of ice on the same scale as the polynya that is subject to similar underlying causes.

65   ## 2   Data and Methods

for this study the combined SMOS-SMAP SIT retrieval and SMOS SIT retrieval (for time periods preceding the installment of SMAP) are used as sea ice thickness of ice above Maud Rise. In addition, the ARTIST sea ice (ASI) algorithm is used to access sea ice concentration and ERA5 meteorological reanalysis data is used to look at winds on the surface level.

2.1   SMOS-SMAP Sea Ice Thickness Retrieval

70   The space-borne passive microwave sensors Soil Moisture Ocean Salinity (SMOS) and Soil Moisture Active Passive (SMAP) are working at 1.4 GHz (L-band) which allows to provide information on the thickness of thin sea ice (SIT). (Paţilea et al., 2019; Huntemann et al., 2014; Tian-Kunze et al., 2014). From modeling and observations it has been established that emission at L-band show sensitivity to ice thickness up to about 50 cm (Kaleschke et al., 2010). The atmosphere has negligible influence on surface emission at L-band (Zine et al., 2008; Kaleschke et al., 2013). The footprint size of both sensors is around 40 km

75   (Paţilea et al., 2019).

The SMOS-SMAP SIT retrieval builds upon its predecessor SMOS SIT retrieval (Huntemann et al., 2014). The SMOS SIT retrieval uses the average of horizontally and vertically polarized brightness temperatures as well as the polarisation difference (i.e., the difference between horizontally polarized and vertically polarized brightness temperature) averaged over the incidence angle range between 40° and 50° from the synthetic aperture antenna observations. SMAP, on the other hand,

80   uses a real aperture antenna and observes the earth surface at a fixed incidence angle of 40° resulting in a narrower swath than SMOS (Paţilea et al., 2019). The combined SMOS-SMAP thin ice sea ice thickness retrieval improves the SMOS retrieval by adapting it to SMAP by modifying it to use fixed 40° incidence angle observations instead of average in the range 40 to 50°. This is achieved by fitting a function to the brightness temperature to incidence angle relation for all overflights of a geographic location of one day. In addition, a linear regression between the SMOS and SMAP brightness temperatures at a 40° incidence

85   angle is performed to align the brightness temperatures of the two instruments with a mean square difference (RMSD) at horizontal and vertical polarization of 2.7 and 2.81 K, respectively (Paţilea et al., 2019). The combined SIT retrieval offers more stable sea ice thicknesses less influenced by Radio-frequency interference (RFI). Because of to the 12 hour difference in the Equator crossing time between SMAP and SMOS, ice thicknesses retrieved from the daily mean brightness temperatures, are more likely to include more the brightness temperature variations within a day which also helps the stability of the retrieval.

90   Therefore, we prefer the use of the combined SMOS-SMAP SIT retrieval above the SMOS-only one for the study of SIT over Maud Rise in cases when it is available.

Both these retrievals were derived from growing sea ice in the Arctic. Only minor evaluation tests have taken place for the Antarctic, where the SIT retrieval was compared with SIT measurements from the EM-bird instrument. The EM-bird is a tethered electromagnetic sensor towed by a helicopter at 15 m above the ice surface operated by Alfred Wegener Institute for Polar and Marine Research. While being on the upper end of the ice thickness sensitivity, the measurements agreed within the given uncertainty of the product, meaning 30%. However, the retrieval does not take into account subtle differences that distinguish the two polar environments. Nevertheless, recently research done on Antarctic phenomena have made use of the SMOS SIT retrieval (e.g., Shi et al., 2021), and more specifically, SMOS SIT retrieval has been used for studying Antarctic polynya (e.g., Heuzé and Aldenhoff, 2018; Mohrmann et al., 2021).

Sea ice concentration (SIC) data (Section 2.2) is necessary to further validate and distinguish SIT data. The SMOS-SMAP retrieval algorithm assumes near-100% SIC when retrieving SIT and since we look at a region prone to polynya and low SIC (Lindsay et al., 2004), it is necessary to consider this factor. The SMOS-SMAP SIT retrieval has no SIC dataset correction implemented because uncertainty of SIC algorithms at high concentration and their covariation at thin thicknesses will cause high errors (Paţilea et al., 2019). Using SIC maps and data in combination with SIT counterparts, we can better infer the location and degree of error in our SIT retrieval. Paţilea et al. (2019) mention specific examples and ratios for the retrieval like sea ice concentration of 90% at 10 cm ice thickness for which the retrieved sea ice thickness is 8.5 cm. Meanwhile, 50 cm ice thickness at 90% sea ice concentration is just 28 cm. Conclusively, all sea ice concentration algorithms show less than 100% SIC for thicknesses below 30 cm (Paţilea et al., 2019). Thus, thin ice thickness data shown in this study should rather be interpreted as a combined ice area and thickness anomaly and not be used to calculate the actual ice volume for the polynya area. However, when the polynya opens, the large heat loss from the ocean often causes thin sea ice to grow, which soon shows up as 100% SIC but will be correctly shown as large-scale thin ice area in the SMOS-SMAP dataset.

2.2 ASI Ice Concentration Algorithm

The ARTIST Sea Ice (ASI) algorithm retrieves SIC from the difference between brightness temperatures at 89 GHz at vertical and horizontal polarizations. This polarization difference is then converted into SIC using pre-determined fixed values for 0% and 100% SIC polarization differences known as tie points. It is known from surface measurements that the polarization difference of the emissivity near 90 GHz is similar for all ice types and much smaller than for open water (Spreen et al., 2008). At such high frequency, atmospheric influence is high also. This effect is dealt with in a bulk correction for atmospheric opacity and by implemented weather filters over open water. Because the Bootstrap (BBA) (Comiso et al., 1997) algorithm uses the 18 and 37 GHz channels, which are less sensitive to atmospheric phenomena, it is also used to essentially filter the produced ASI SIC concentration by setting SIC to zero where the Bootstrap algorithm retrieves less than 5% SIC.

2.3 ERA5 Climate Reanalysis

ERA5 Climate Reanalysis data is used to study direct atmospheric forcing on the opening of the polynya as well as on anomalous regional sea ice thinning to conclusively answer whether the Weddell Sea Polynya is purely ocean-driven or maintained by a combination of both processes.

125   ECMWF Reanalysis 5th Generation (ERA5) embodies a detailed record of the global atmosphere, land surface and ocean
from 1950 onwards. It replaces the ERA-Interim reanalysis (spanning 1979 onwards) and is based on the Integrated Forecasting
System (IFS) Cy41r2. ERA5 benefits from a decade of developments in model physics, core dynamics and data assimilation
(Hersbach et al., 2020). In addition to a significantly enhanced horizontal resolution of 31 km, compared to 80 km for ERA-
Interim, ERA5 has hourly output throughout, and an uncertainty estimate from a 10-member ensemble of data assimilations
130   with 3-hourly output.

   Campbell et al. (2019) report that there exist a high degree of similarity between six-hourly mean sea level pressure (MSLP)
from SANAE-AWS weather station, south of Maud Rise, and the nearest ERA-Interim grid cell from 1997 to 2019 ($r = 0.93$;
mean absolute deviation $= 2.2\,\mathrm{hPa}$; mean bias $= 0.8\,\mathrm{hPa}$). On these grounds, ERA-I was deemed accurate for gathering signs
of storm activity as it skillfully represented MSLP variability near Maud Rise. ERA5 is a reanalysis with a higher temporal
135   and spatial resolution than ERA-I. It improves upon its predecessor in terms of information on variation in quality over space
and time as well as an improved troposphere modelling. As a result, for the purposes of this study, it should offer a better, or
at least identical, assessment of the wind speeds near Maud Rise that are going to be cross-referenced with the presented SIT
retrievals in this study.

3   Results

140   Figure 1 shows the full 11-year record of SMOS sea ice thickness from 2010 to 2020 above Maud Rise. For a detailed analysis
of the Weddell Sea Polynya, the two years September 2017 and September 2018 were chosen. The full 11-year time series
will be discussed at the end of the result section. In 2017 the polynya shows the the largest extent and is open the longest time
period, in 2018 the polynya is visible as sea ice thickness anomaly but does not open completely (Fig. 1). Here the advantage
of the SMOS-SMAP ice thickness retrieval shows its strength compared to the traditional sea ice concentration datasets. This
145   section presents findings that suggest a previously unrecognized similarity between the two September anomalies.

   Fig. 2 shows a standard Southern Hemisphere SMOS-SMAP SIT retrieval at grid resolution of 12.5 km with a total of 664
rows and 632 columns. The black frame (62 to $67.5°$S,-3.5 to $9°$E), which shows austral winter sea ice above Maud Rise
($66°$S,$3°$E), is the same area as the smaller 2018 maps in Fig. 2 as well as all 2017 maps in Fig. 3. Accompanying the SMOS-
SMAP 2017 maps are the ASI SIC counterparts at nominal resolution of 6.25 km covering the same segment for comparison.
150   The 2017 Weddell Sea Polynya is a well-documented event and its preconditioning as well as existence until melt of that
year has been shown via satellite imagery; most commonly via SIC retrieval (e.g., Campbell et al., 2019). Here the advantages
of SMOS-SMAP SIT retrieval are limited by the high open water fraction but nevertheless help to demonstrate the full extent
of the anomaly that SIC maps of the region can only partially depict (see Fig. 3).

   August and September 2018, shown in the time series plots of Fig. 4, is the time period of interest for this research, where
155   the polynya is visible as SIT anomaly but does not open. Looking at the SIT record for the two months (Fig. 4c), we can see
the area thinner than $50\,\mathrm{cm}$ (brown line) exceeds $250 \cdot 10^3$ km^2 (17-20 Sep) and ice thinner than $20\,\mathrm{cm}$ (green line) is detected
on multiple days (8–12 Sep, 16–19 Sep) in an anomaly spanning almost the entirety of September. SIC time series (Fig. 4b)
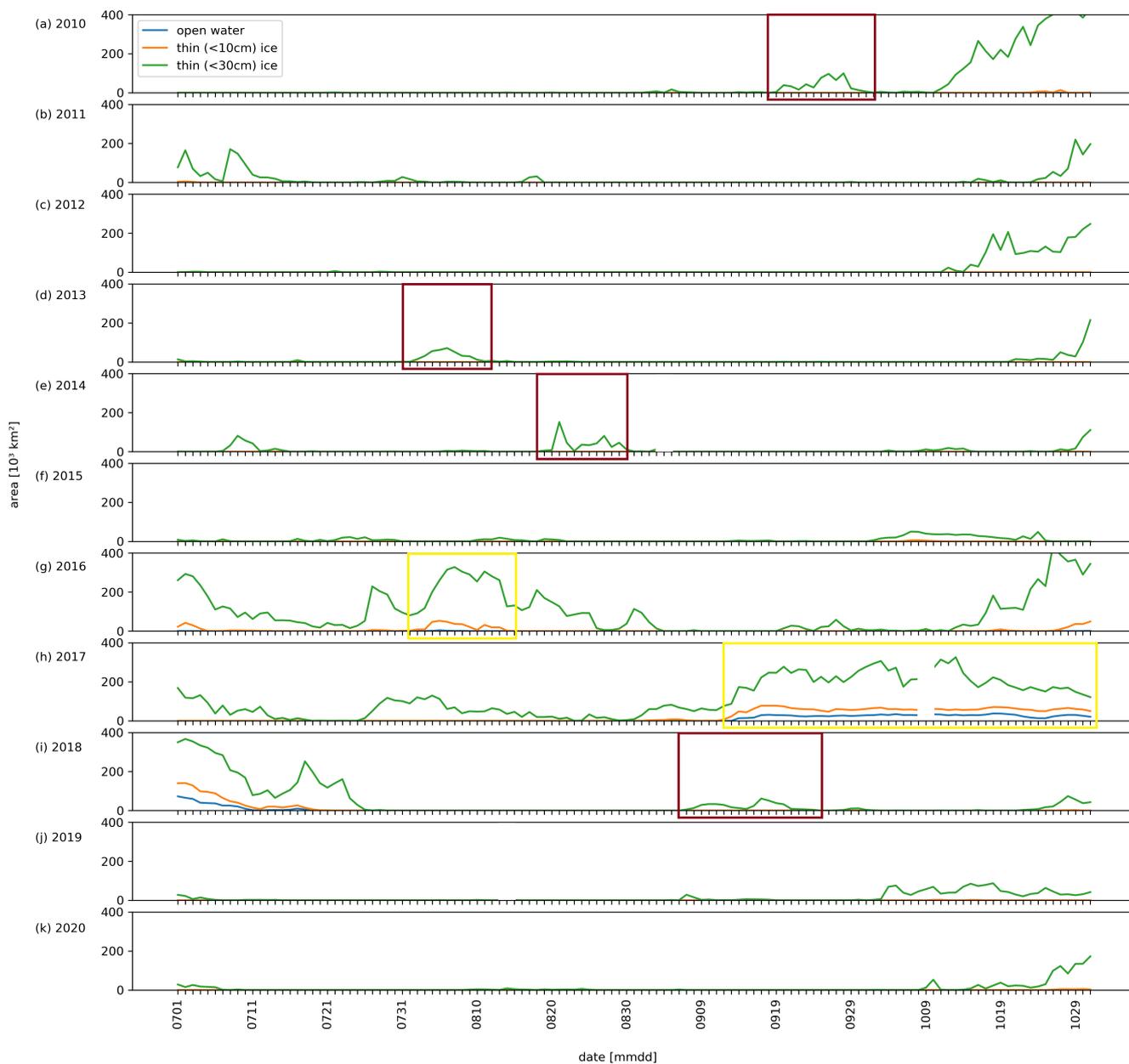
Figure 1. (a-k) the SMOS SIT retrieval time series from 2010 to 2020 over the area of interest outlined in Fig. 2. As with SMOS-SMAP SIT retrieval time series, each line represents the area of sea ice below a thickness threshold shown in the legend in the top left (blue: open water, orange: <10 cm, green <30 cm). Polynya events are highlighted in yellow whereas ice thinning anomalies are highlighted in red. Years 2017 and 2018 are discussed in more detail in this manuscript.
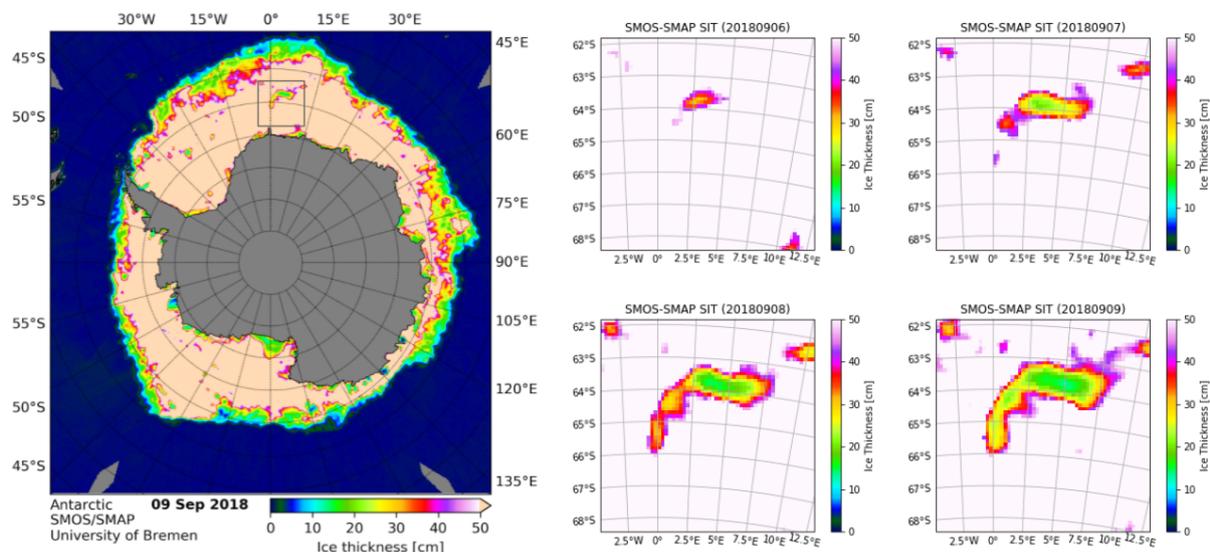
Figure 2. Left: SMOS-SMAP SIT retrieval spanning the Antarctic continent and surrounding regions. The segment contained in the black square depicts sea ice above Maud Rise (66°S,3°E). Right: the local SMOS-SMAP SIT of the outlined segment is shown on four different days: 6-9 September 2018.
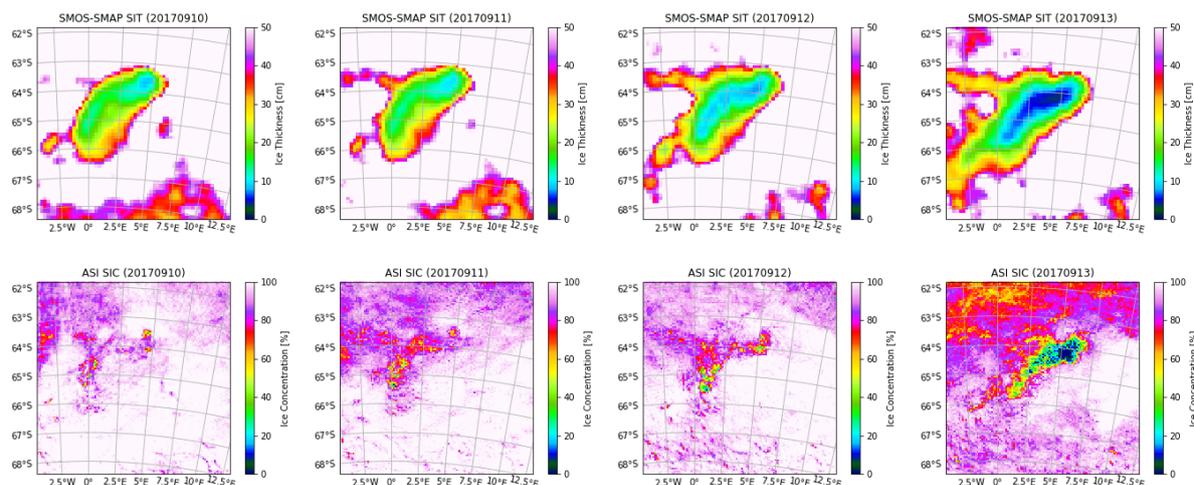
Figure 3. SMOS-SMAP SIT (top row) and ASI SIC (bottom row) retrieval of the days leading up the 2017 Weddell Sea Polynya: 10-13 September 2017.

seems to vaguely reflect the SIT anomaly of late September by sporadic episodes of below 80% SIC (purple line) but does not describe the anomaly like the SIT record does. No SIC area below 40% is detected and thus no significant open water area
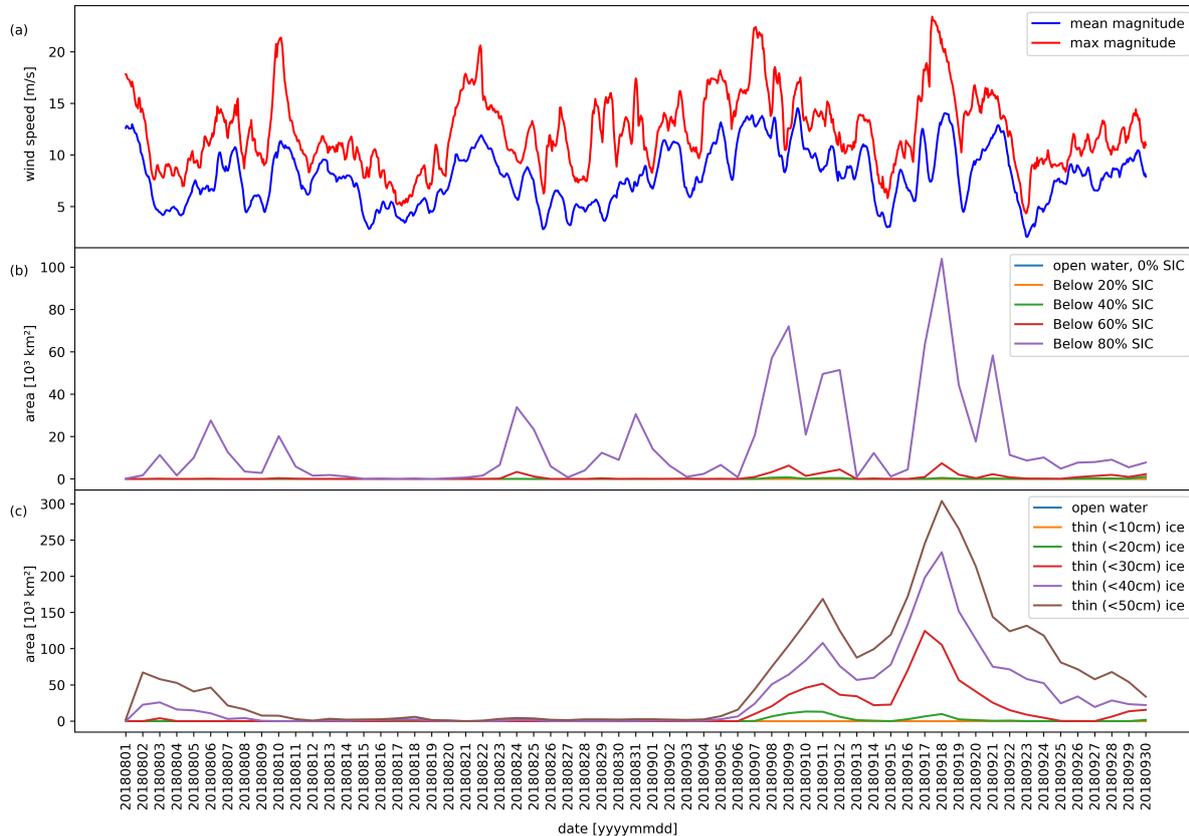
Figure 4. August–September 2018: (a) Daily ERA5 wind speed (red: daily maximum; blue: mean). (b) ASI SIC where each line represents the area of sea ice that falls below a SIC value shown in the legend. (c) SMOS-SMAP SIT where each line represent the area of sea ice below a thickness shown in the legend. All plots cover the area of interest outlined in Fig. 2.

160   prevailed that year. Atmospheric data (Fig 4a) in the form of wind speed derived from u and v components of wind velocity vectors are presented as daily average (in blue) and maximum (in red) magnitude in the region of interest. Notably we can see the highest mean (9–10 Sep) at the start of the SIT anomaly and the highest maximum at the same time as the peak of the anomaly (17–18 Sep). Thus wind could have contributed to the formation of the 2018 "polynya thin ice" event.

Fig. 5 depicts the Weddell Sea Polynya of 2017 from its preconditioning to its formation up until the end of September.
165   Interpreting the wind speed results shown in Fig. 5a as compared to the lower polynya area and thickness plots, we see that the highest maximum (in red) and mean (in blue) wind speed magnitude both coincide with the 13 September polynya opening date. From the ASI SIC record (Fig. 5b), we can see both the similarities it shares with the SIT record (Fig. 5c) as well as clear differences that will be further discussed below. Important to note is that the blue line in both SIC and SIT records represents the area that is classified as open water. These lines are also present in the 2018 Fig. 4b and 4c but are consistently at $0\,\mathrm{km}^2$
170   and therefore hidden because of the overlap with low SIC and low SIT lines.

8
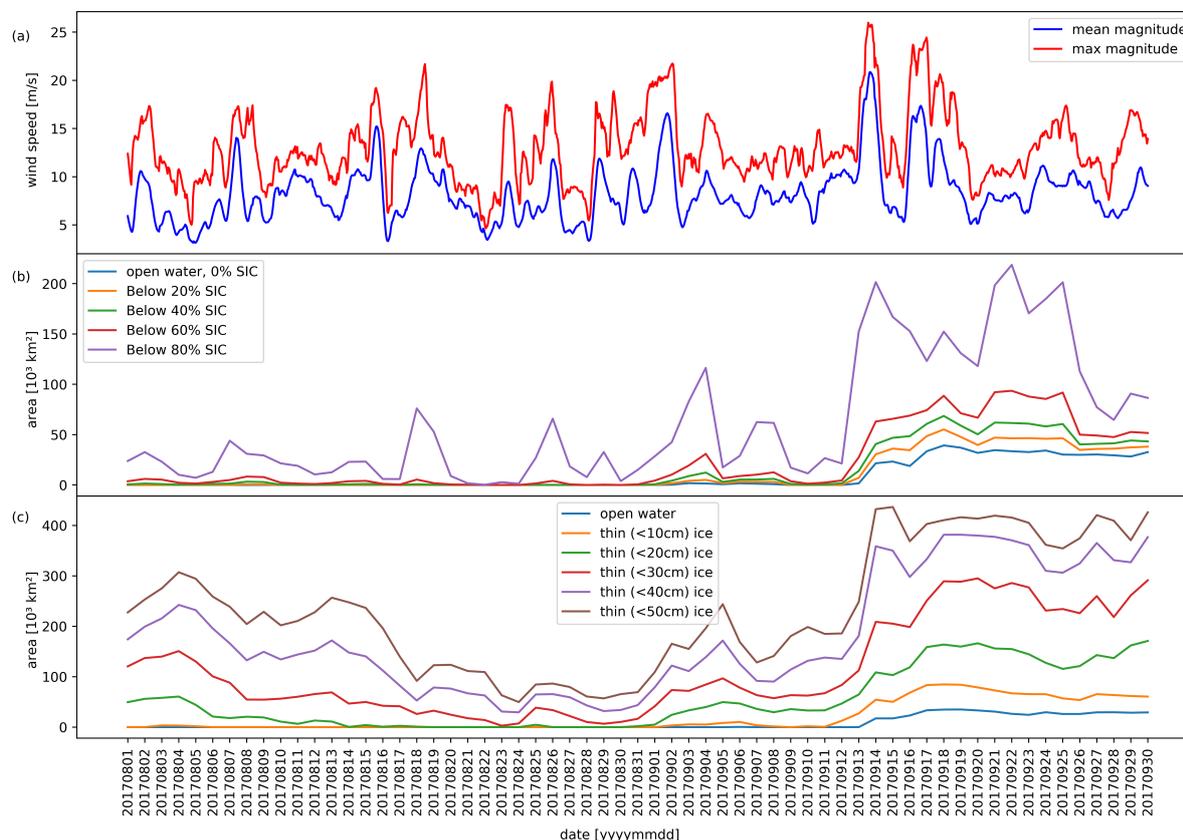
Figure 5. August–September 2017: (a) Daily ERA5 wind speed (red: daily maximum; blue: mean). (b) ASI SIC where each line represents the area of sea ice that falls below a SIC value shown in the legend. (c) SMOS-SMAP SIT where each line represent the area of sea ice below a a thickness shown in the legend. All plots cover the area of interest outlined in Fig. 2.

In Fig. 1 we show the entire 11-year SMOS record in the form of a time series. For the highlighted regions, maps of the ice anomaly are shown in Fig. 6. Time frames highlighted in yellow are the 2016 and 2017 Weddell Sea Polynya events whereas red frames surround the periods of ice thinning anomalies. Note that while the two polynya events are unique in the extended time series, ice thinning anomalies seem to have a higher frequency of occurrence.

3.1 Discussion

The polynya maps in Fig. 2 and Fig. 3 are useful for accessing fine details of low SIT distributions as well as comparing SIT retrieval with ASI SIC (Fig. 3). By capturing the low sea ice thickness anomaly in 2018 and at the beginning of the 2017 polynya event in the SIT record we can infer that there were residual polynya-favourable effects that produced a forcing that was insufficient to open the polynya but sufficient to still impact the overlying sea ice. This is similar to the 1970s polynya cases, where the 1973 polynya resulted in a much larger iteration of the Weddell Sea Polynya visible from 1974 to 1976. Cheon
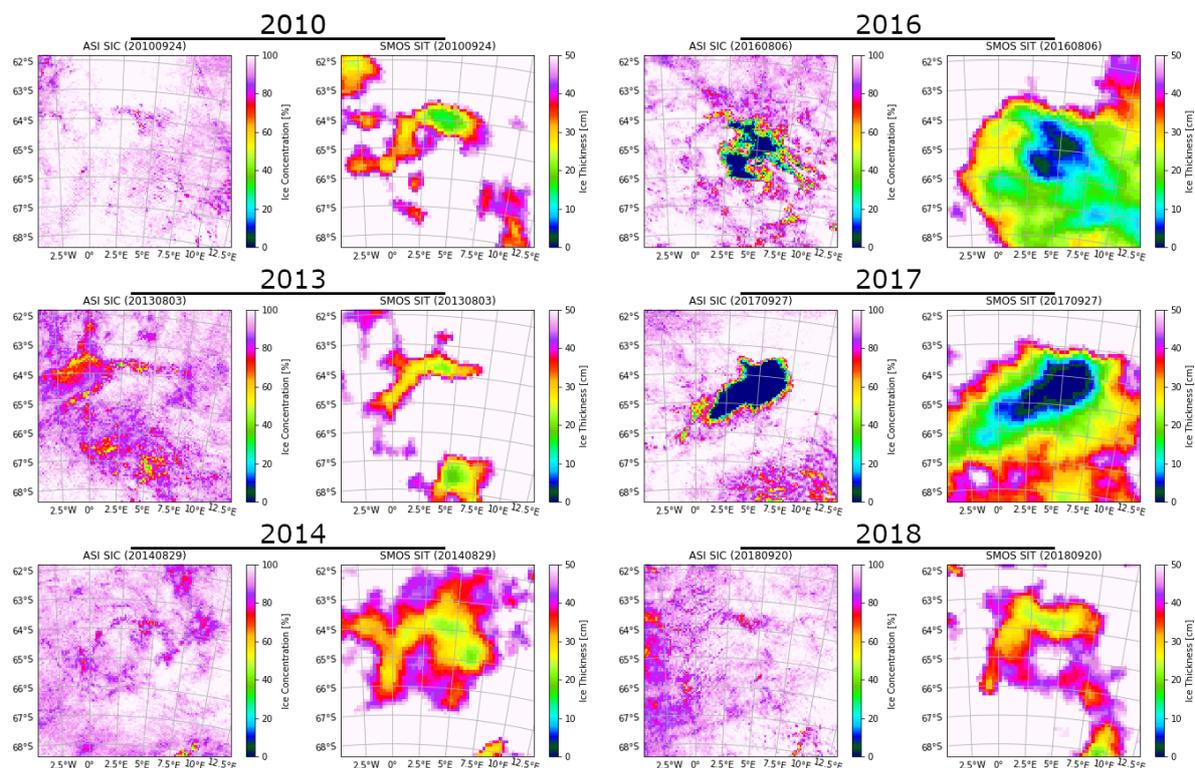
Figure 6. ASI SIC and SMOS SIT retrieval maps covering all major thinning events that can be seen in the 11-year SMOS record (Fig. 1).

and Gordon (2019) attribute the lack of any polynya in 2018 in part to the positive state of the Southern Annular Mode inducing fresh surface water conditions effectively capping warmer deep water convection and the weakening of the Weddell Gyre in the years that followed its peak activity in 2015 and 2016. This study aims to present a more plausible scenario where rather than an abrupt change from the largest Weddell Sea Polynya in 2017 to lack thereof we have a waning of this phenomenon with peak activity in 2017.

In order to analyse the time periods during which the polynya of 2017 (Fig. 5) and the sea ice anomaly of 2018 (Fig. 4) occurred, we view the respective time series. 2017 in Fig. 5c shows a progression of events in terms of SIT of how the polynya came to be. First and foremost we have a major regional ice thinning early August that peaks on the fourth of August much like the minor Weddell Sea Polynya of 2016 that also peaked on 4-5 August of that year (see Fig. A1 in the appendix). Looking at 5b we can see how much smaller the area affected by SIC variations is and how it is different in behaviour to the SIT time series. Only the "below 80%" SIC shows some variability, however, not very correlated to the SIT time series. This is especially true during the brief period (6-12 Sep) leading up to the polynya, which is promising because it suggests a lack of low SIC-induced SIT values due to the SMOS-SMAP SIT retrieval full ice cover assumption. In total, compared to the $50 \cdot 10^3$ km^2 of below 100% SIC area, less than 50 cm thick ice spans over $300 \cdot 10^3$ km^2 of the region of interest. Following the period mentioned (6-12 Sep), we have the sudden peak (12-13 Sep) in both lower sea ice concentrations and thin sea ice. Based on Fig. 3, we see

10

that this, at first minor opening in sea ice, paved way to the Weddell Sea Polynya. From an oceanographic point of view this would imply heat exchange with the atmosphere which would cool the surface water layer and destabilize the water column. This destabilization, further facilitated by the effect of the Taylor column, isolates the water mass above Maud Rise (Muench et al., 2001). The lack of stratification in the waters surrounding the Antarctic continent, would trigger convection cells able

200   to bring up warm Deep Water from below. In Fig. 3 we can see the much larger scale effect this is having on SIT rather than SIC and how peaks of low SIC and low SIT do not coincide in Fig. 5b and Fig. 5c, respectively. Instead, we see the low SIT area peak occurring 5-6 September following the 4 September peak in low SIC area which is what we expect considering how the convection cell would not simply cease immediately after the the smaller openings in ice freeze up; but rather its effects would be "felt" in the general location for days to come. With the ocean destabilized, coupled with heavy storm activity as can

205   be seen in Fig. 5a by wind speeds reaching 25 m/s, we see the polynya open on 13 of September 2017.

    Fig. 4 shows that 2018 is less anomalous than 2017 for the first one and half months until the sea ice anomaly begins to form on the 6 of September 2018. There is an initial thinning and occasional sporadic "below 80%" SIC events distributed throughout the period. Notably, the event on 24 August and 31 August, seen in Fig. 4b seem to suggest lead openings in thick pack ice as there is no thinning recorded in the SIT retrieval for those days. The sea ice anomaly itself, as can be seen in Fig. 4c, is very

210   well defined in the SIT record and has a clear beginning and an end. Notable is that the two consecutive low SIT area peaks are characterised by more extreme case of thinning during the first smaller peak reaching a prolonged period (7-13 September) of ice thinner than 20 cm followed by a much larger area of ice thinner than 50 cm (15-21 September). This anomaly follows a period of relatively strong mean and maximum wind speed from 3 August to 13 Sep towards the East and Southeast directions (Fig. 4) that could imply that wind-driven ice advection influences the sea ice anomaly as any attempt at refreezing ice that has

215   been broken apart by wind would require newly formed thin ice. Similarly, low SIC and strong winds would enhance heat loss from the ocean and cause upwelling warm water, which would melt the ice from below. Fig. 7 depicts hourly wind conditions during the start of the sea ice anomaly on 7 September 2018: the strong westerly winds (blowing towards the East) common for this region occasionally show a more northerly component roughly where the sea ice anomaly began to form at the same time.

220   Through the comparison of our SIC data with ERA5 atmospheric data we can infer when wind can force the Weddell Sea Polynya to open and when it cannot. Fig. 8 show the wind conditions on 13 September 2017 where for several hours strong winds (20 m/s) prevailed above the region of interest suggesting heavy storm activity. In contrast, regional winds in September 2018 are consistently below 15 m/s (mean) and areas of strong wind seem to be localised around rather than on top of Maud Rise. It is hard to say whether stronger storms during the sea ice anomaly of 2018 would have caused a polynya to open as it is

225   not known quantitatively how much different factors contribute to the formation of the polynya. But it is clear that atmospheric forcing is a strong contributing factor especially towards the start of the polynya. Thereafter also oceanic upwelling of warm water due to the reduced stratification plays an increasing role.

    Lastly, we use the SMOS SIT retrieval instead of the combined SMOS-SMAP to analyze years before 2015 (the year when SMAP was put into orbit) to make a consistent 11 year SIT time series over the months of July, August, September and October

230   (Fig. 1) to fully include the freezing periods of the relevant region over the years. Notably, the sea ice thinning of 2018 is by
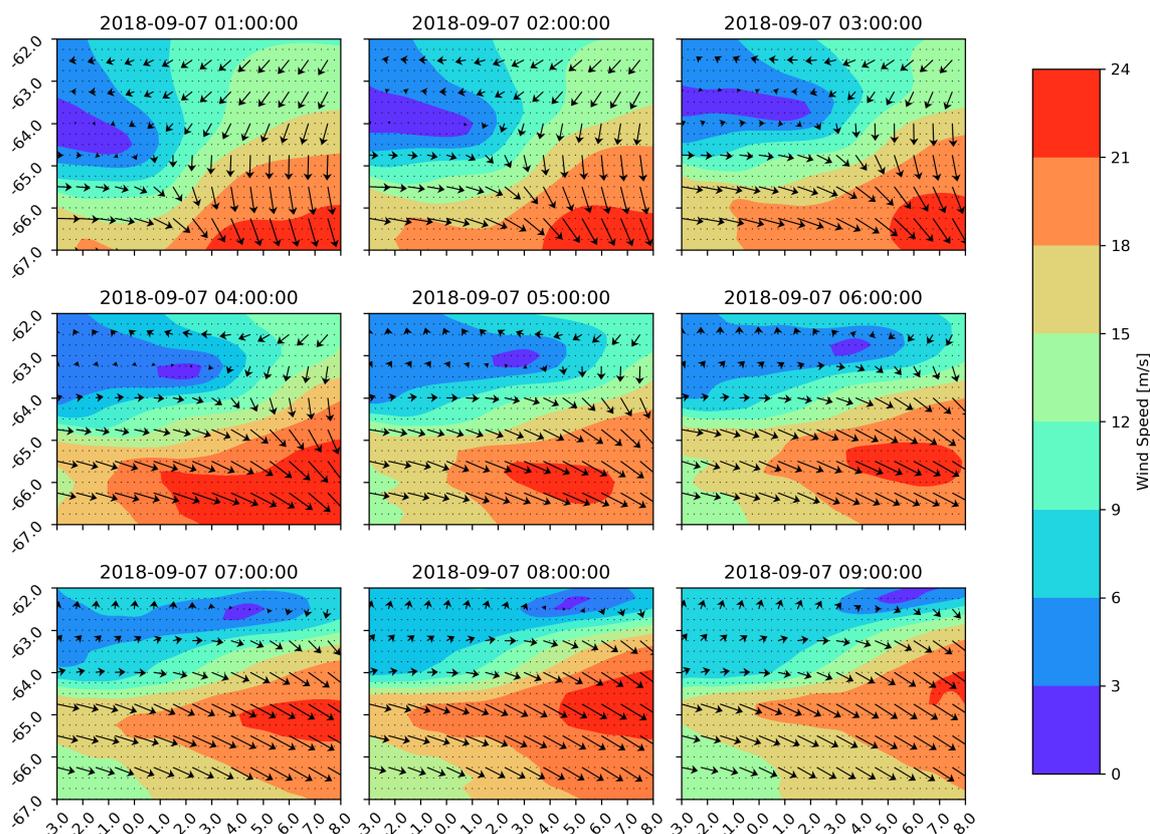
Figure 7. ERA5 quiver and contour plots of wind activity above Maud Rise on 7 September 2018, the day the 2018 sea ice anomaly starts to form. All plots cover the area of interest outlined in Fig. 2.

no means an isolated event and the Maud Rise region seems to be regularly subject to sea ice thinning events. While the SIC record offers two prominent anomalous events: the Weddell Sea Polynya of 2016 and 2017, respectively (highlighted in yellow in Fig. 1), it is through the SIT retrieval that we identify all other anomalies that have occurred over the years. Specifically, years in which the polynya did not occur but still showed signs of ice thinning are 2010, 2013, 2014 and 2018 (not counting

235   thinning episodes that follow freeze-up or precede melt); they are highlighted in red in Fig. 1. In Fig. 6, we look specifically at the events highlighted in Fig. 1 to get a better picture of ice thinning anomalies and polynya throughout the 11-year SMOS record. The similarities of these anomalous events further consolidate the idea of many polynya-favourable events taking place in the region with each having their own effect on the ice cover.
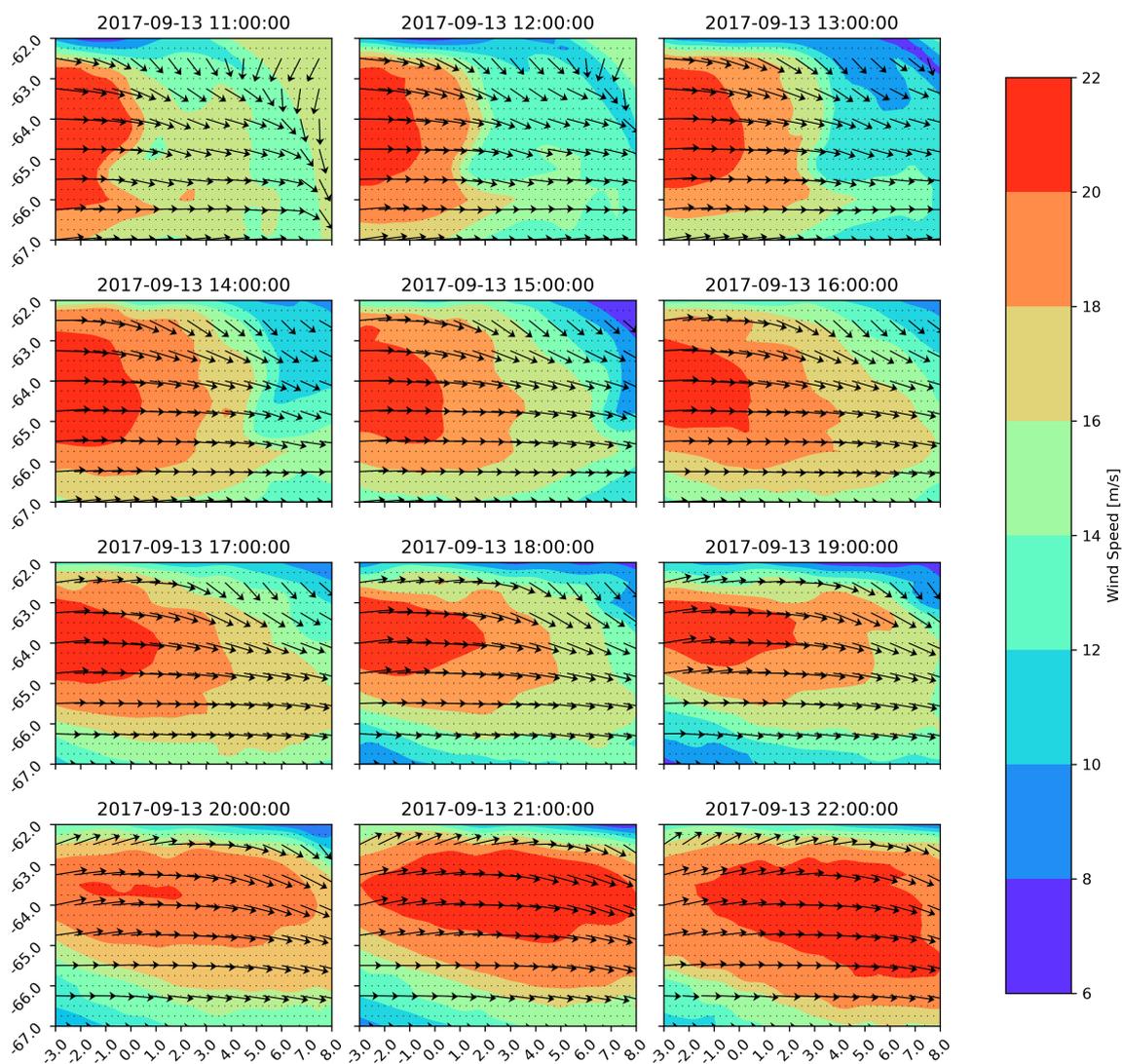
Figure 8. ERA5 quiver and contour plots of wind activity above Maud Rise on 13 September 2017, the day the 2017 Weddell Sea polynya opens. All plots cover the area of interest outlined in Fig. 2.

4   Conclusions

240   From the SIC data product it is known that a Weddell Sea Polynya events occurred in August 2016 (3-9 Aug) and September 2017 (13 Sep until melt of that year), respectively. From the SMOS-SMAP SIT record we now know that anomalous episode of sea ice above Maud Rise spans a wider time span than previously assumed. With the sea ice anomaly of 2018 (5-30 Sep) as well as thinning events in 2010, 2013 and 2014 that can be identified in Fig. 1, we can conclusively say that anomalous "polynya-type" behaviour was much longer than anticipated and is indicative of a more regular pattern of thin sea ice in the

245   region.

By analysing the three different data products (SIT, SIC and ERA5 meteorological reanalysis) and comparing them with one another, we have answered the two principal questions of this study: whether atmospheric forcing influences the sea ice region above Maud Rise and more importantly, whether SIT retrieval is a viable candidate for the study of the Weddell Sea Polynya. As expected direct atmospheric forcing is very much involved in wide-scale drops in SIT and SIC above Maud Rise,

250   in addition to oceanographic forcing. This, although not new (e.g., Campbell et al., 2019; Heuzé and Lemos, in review, 2020), is not universally accepted. Rather most rigorous explanations behind the processes that cause the Weddell Sea Polynya do not include direct atmospheric forcing, rather indirect large-scale atmospheric involvement is mentioned in the form of the negative wind stress curl intensifying the Weddell Gyre (Cheon and Gordon, 2019). What is more, we are also able to link wind activity with the sea ice anomaly of 2018, a year that unlike its recent predecessors had one of the coldest ocean temperature profiles

255   (Cheon and Gordon, 2019). Cheon and Gordon (2019) report that heat loss from the ocean over the span of both the 1973-1976 polynya events as well 2016-2017 is quite high. That is to be expected as sea ice acts as an efficient insulator between the two mediums. However, this in turn gives more precedence to atmospheric forcing being the dominant factor in both the thinning of 2018 and opening of the polynya on 13 September 2017. Important to note is that for this study also other parameters were calculated from the base ERA5 data products like atmospheric divergence and curl (not shown), which have also been used to

260   identify direct atmospheric forcing (Heuzé and Lemos, in review, 2020). In the end, strength of the wind magnitude present above the region has the most direct correlation with drops in SIT and SIC. Even more than the wind direction, which although sporadic, is generally towards the East as the area is dominated by westerlies. Also worth mentioning is the work done by Francis et al. (2020) that demonstrate the impact of atmospheric rivers during polynya years which carry with them latent heat that aid cyclone formation. As such, along with other polynya-favourable conditions like cloud cover (Francis et al., 2020),

265   atmospheric rivers are yet another process that aid in the formation of the Weddell Sea Polynya. With so many processes driving the formation of the polynya it is thus no surprise to see more regularity in sea ice anomalies in the region, as the 11-year SIT time series has shown (Fig. 1). However, in most of the years the forcing was not strong enough to open the polynya and only the SIT record shows the imprint of an "polynya-type" event. Moreover, it is the combination of these polynya-favourable forcings that cause the Weddell Sea Polynya but each have their own effect on the sea ice cover.

270   As for effectiveness of SIT analysis, we have demonstrated that it offers information that is unique as compared to standard SIC-based analysis of the region. While influenced by SIC, the SMOS-SMAP SIT retrieval has demonstrated itself as an independent source of information that provides reasonable data about the ice conditions above Maud Rise. Most impressive

are periods of near-100% SIC and low SIT as during pre-polynya periods. When the polynya is open, the SIT signal from the retrieval is unlikely to provide accurate ice thickness data due to large areas of open water influencing the signal. As mentioned
275 before, low SIC affects the SIT record. Other sources of uncertainty can be flooded ice and slush caused by snow pushing down the sea ice such that water floods from the sides or from below through cracks in the sea ice. However, we do not have indication that this happened here. Due to the potential uncertainties in this study the SIT record serves mainly as an indicator of anomalous sea ice activity rather than a means by which to quantify the exact degree of thinning in the region.

In 2018, a polynya-free year, SIT retrieval has shown that the beginning and end of a sea ice anomaly that, at its peak (18 Sep:
280 <50 cm sea ice region with an area of $300 \cdot 10^3$ km^2), reached an estimated area larger than the United Kingdom. It is apparent that the low SIT anomaly covered a much wider area than where low SIC (most likely minor lead openings) is recorded. As such, SMOS-SMAP SIT analysis is a method by which the Maud Rise region can be better monitored on a more frequent basis. This type of analysis, able to detect anomalous activity above Maud Rise with high temporal resolution, paves way to a better understanding of the underlying processes that not only drive the polynya but are in fact affecting the sea ice more often
285 than previously thought possible. An extension of the 11-years SMOS time series is needed to better quantify the regularity and how often such polynya-type ice anomaly events occur. As both SMOS and SMAP are science missions with no planned follow ups there is a chance that we will have a gap in the current L-band radiometry capability in space. However, with the future, operational Copernicus CIMR mission (planned launch 2028; https://cimr.eu/) some continuation of the SIT time series will be possible.

290 In conclusion, the classification of the Weddell Sea Polynya as a purely-open ocean polynya has been challenged and clear links between wind speed magnitude and polynya conditioning have been found. As for SIT retrieval from L-band microwave radiometers like SMOS ad SMAP: it is an effective tool at monitoring sea ice conditions above Maud Rise and capable of collecting more substantial information than its SIC counterpart. Rather than substitute SIC retrieval though, the two should be used in conjunction with one another to aid the scientific understanding of the processes taking place and it should be added as
295 yet another tool at trying to understand the unique and complex processes present in the Maud Rise region.

Data availability. The SMOS–SMAP SIT and ASI SIC daily data are available at https://seaice.uni-bremen.de/databrowser/.

Appendix A

A1   The 2016 Polynya Event

In Fig. A1 we show the 2016 polynya in the same format as the 2017 polynya and 2018 ice thinning anomaly.
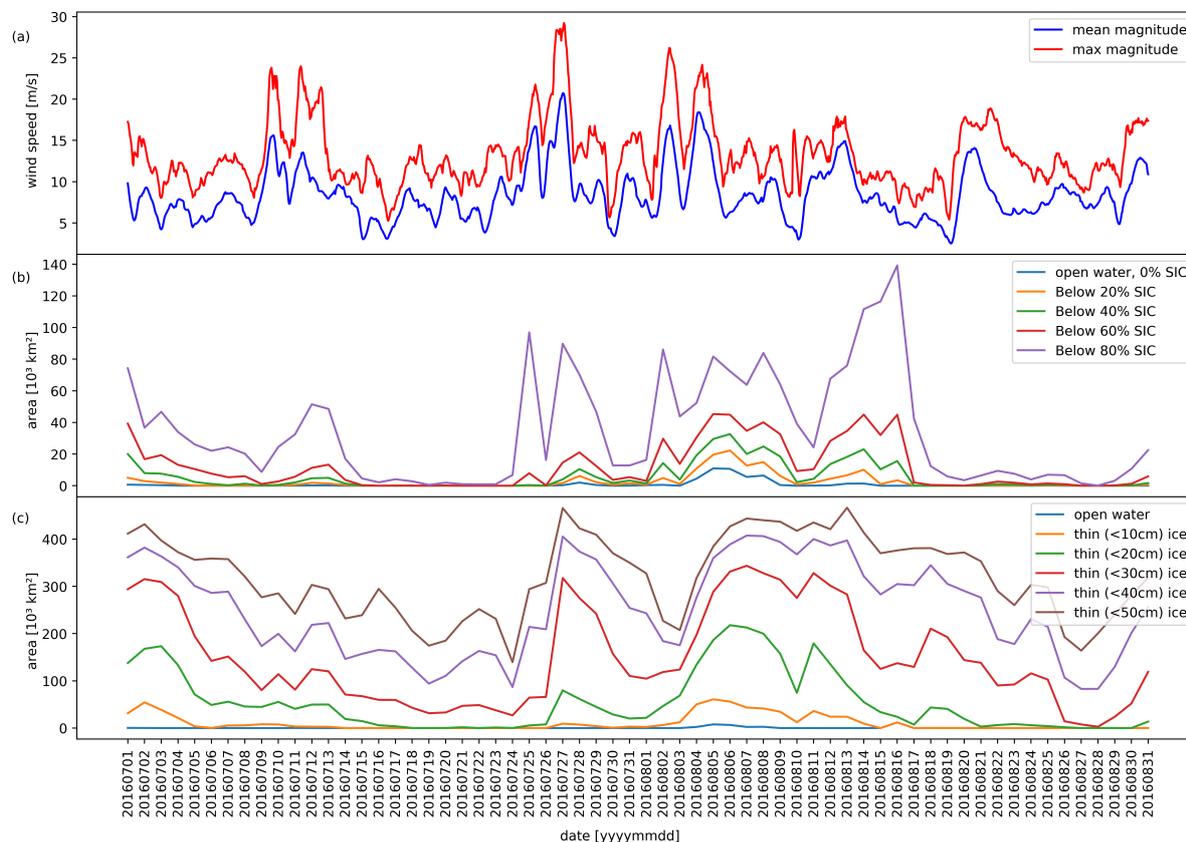
Figure A1. August–September 2016: (a) Daily ERA5 wind speed magnitude (red: daily maximum; blue: mean). (b) ASI SIC where each line represents the area of sea ice that falls below a SIC value shown in the legend. (c) SMOS-SMAP SIT where each line represent the area of sea ice below a thickness shown in the legend. All plots cover the area of interest outlined in Fig. 2.

A2 MODIS comparison

In Fig. A2 we show the Weddell Sea Polynya of 2017 and the sea ice thinning anomaly of 2018 as seen by the MODIS instrument onboard the TERRA satellite (processed and made available through NASA Worldview, https://worldview.earthdata.nasa.gov/).

16
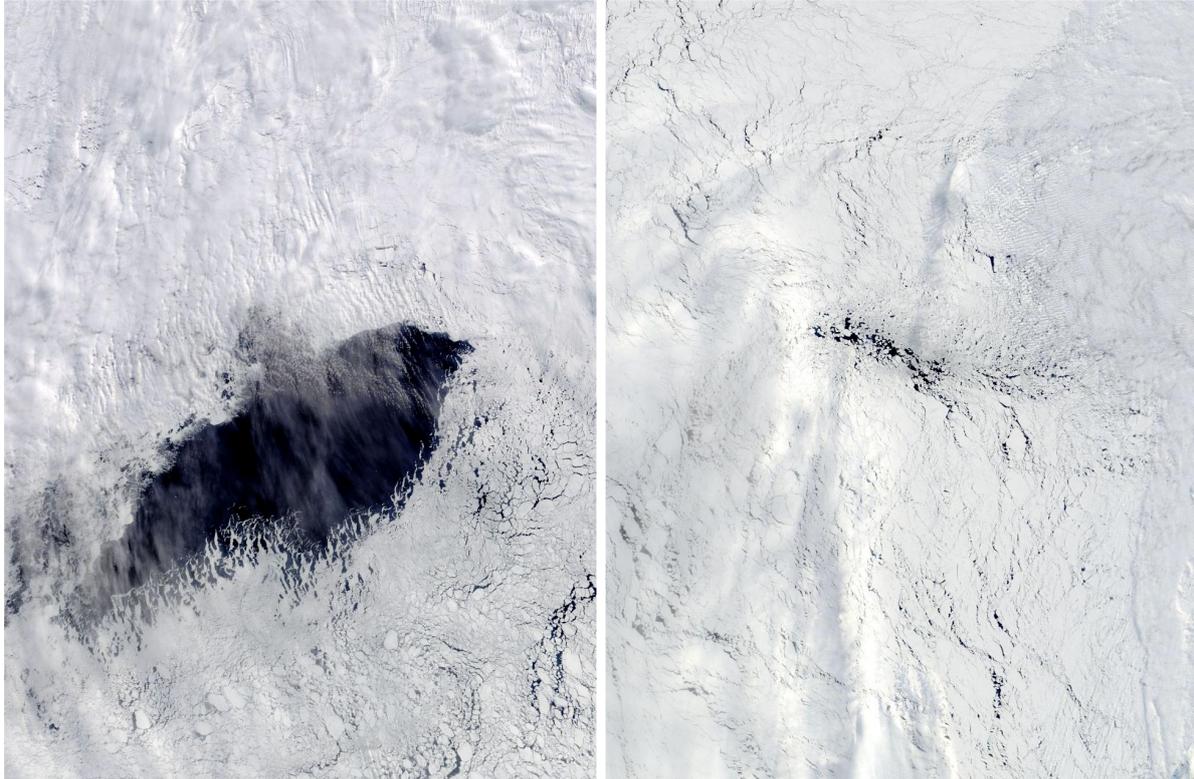
Figure A2. Left: MODIS image of the Weddell Sea Polynya (25 September 2017). Right: MODIS image of the sea ice anomaly of 2018 (8 September 2018). Area viewed in both snippets is the same and chosen by assigning the bottom left corner and top right corner to chosen coordinates upon selection: 67°S, 1°E and 61°S, 8°W, respectively (images from NASA Worldview, https://worldview.earthdata.nasa.gov/).

Competing interests. The authors declare that they have no conflict of interest.

References

Bersch, M., Becker, G. A., Frey, H., and Koltermann, K. P.: Topographic effects of the Maud Rise on the stratification and circulation of the Weddell Gyre, Deep Sea Research, 39, 303–331, https://doi.org/https://doi.org/10.1016/0198-0149(92)90111-6, 1992.

320 Campbell, E. C., Wilson, E. A., Moore, G. W. K., Riser, S. C., Brayton, C. E., Mazloff, M. R., and Talley, L. D.: Antarctic offshore polynyas linked to Southern Hemisphere climate anomalies, Nature, 570, 319–325, https://doi.org/https://doi.org/10.1038/s41586-019-1294-0, 2019.

Cheon, W. G. and Gordon, A. L.: Open-ocean polynyas and deep convection in the Southern Ocean, Scientific Reports, 9, https://doi.org/https://doi.org/10.1038/s41598-019-43466-2, 2019.

325 Comiso, J. C., Cavalieri, D. J., Parkinson, C. L., and Gloersen, P.: Passive microwave algorithms for sea ice concentration: A comparison of two techniques, Remote Sensing of Environment, 60, 357–384, https://doi.org/https://doi.org/10.1016/S0034-4257(96)00220-9, 1997.

Francis, D., Mattingly, K. S., Temimi, M., Massom, R., and Heil, P.: On the crucial role of atmospheric rivers in the two major Weddell Polynya events in 1973 and 2017 in Antarctica, Sci Adv, 6, https://doi.org/https://10.1126/sciadv.abc2695, 2020.

Hersbach, H., Bell, B., Berrisford, P., Hirahara, S., Horányi, A., Muñoz-Sabater, J., Nicolas, J., Peubey, C., Radu, R., Schepers, D., Simmons,
330 A., Soci, C., Abdalla, S., Abellan, X., Balsamo, G., Bechtold, P., Biavati, G., Bidlot, J., Bonavita, M., Chiara, G. D., Dahlgren, P., Dee, D., Diamantakis, M., Flemming, R. D. J., Forbes, R., Fuentes, M., Geer, A., Haimberger, L., Healy, S., Hogan, R. J., Hólm, E., Janisková, M., Keeley, S., Laloyaux, P., Lopez, P., Lupu, C., Radnoti, G., de Rosnay, P., Rozum, I., Vamborg, F., Villaume, S., and Thépaut, J.: The ERA5 global reanalysis, Quarterly Journal of the Royal Meteorological Society, 146, 1999–2049, https://doi.org/https://doi.org/10.1002/qj.3803, 2020.

335 Heuzé, C. and Aldenhoff, W.: Near-Real Time Detection of the Re-Opening of the Weddell Polynya, Antarctica, from Spaceborne Infrared Imagery, IEEE, https://doi.org/https://doi.org/10.1109/IGARSS.2018.8518219, 2018.

Heuzé, C. and Lemos, A.: Spaceborne infrared imagery for early detection and cause of Weddell Polynya openings, The Cryosphere Discuss, https://doi.org/https://doi.org/10.5194/tc-2020-123, in review, 2020.

Huntemann, M., Heygster, G., Kaleschke, L., Krumpen, T., Mäkynen, M., and Drusch, M.: Empirical sea ice thickness retrieval during the
340 freeze-up period from SMOS high incident angle observations, The Cryosphere, 8, 439–451, https://doi.org/https://doi.org/10.5194/tc-8-439-2014, 2014.

Jena, B., Ravichandran, M., and Turner, J.: Recent Reoccurrence of Large Open-Ocean Polynya on the Maud Rise Seamount, Geophysical Research Letters, 46, https://doi.org/https://doi.org/10.1029/2018GL081482, 2019.

Kaleschke, L., Maaß, N., Haas, C., Hendricks, S., Heygster, G., , and Tonboe, R. T.: A sea-ice thickness retrieval model
345 for 1.4 GHz radiometry and application to airborne measurements over low salinity sea-ice, The Cryosphere, 4, 583–592, https://doi.org/https://doi.org/10.5194/tc-4-583-2010, 2010.

Kaleschke, L., Tian-kunze, X., Maaß, N., Heygster, G., Huntemann, M., Wang, H., Hendricks, S., Krumpen, T., Tonboe, R., Mäkynen, M., and Haas, C.: ESA Support To Science Element (STSE) SMOS Sea Ice Retrieval Study (SMOSIce) Final Report ESA ESTEC Contract No .: 4000101476 / 10 / NL / CT, Tech. rep., University of Hamburg, 2013.

350 Lindsay, R. W., Holland, D. M., and Woodgate, R. A.: Halo of low ice concentration observed over the Maud Rise seamount, Geophysical Research Letters, 31, https://doi.org/https://doi.org/10.1029/2004GL019831, 2004.

Mohrmann, M., Heuzé, C., , and Swart, S.: Southern Ocean polynyas in CMIP6 models, The Cryosphere Discuss, https://doi.org/https://doi.org/10.5194/tc-2021-23, 2021.

Muench, R. D., Morison, J. H., Padman, L., Martinson, D., Schlosser, P., Huber, B., and Hohmann, R.: Maud Rise revisited, Journal of

355   Geophysical Research: Oceans, 106, 2423–2440, https://doi.org/https://doi.org/10.1029/2000JC000531, 2001.

Pațilea, C., Heygster, G., Huntemann, M., and Spreen, G.: Combined SMAP–SMOS thin sea ice thickness retrieval, The Cryosphere, 13, 675–691, https://doi.org/https://doi.org/10.5194/tc-13-675-2019, 2019.

Shi, Q., Su, J., Heygster, G., Member, IEEE, Shi, J., Wang, L., Zhu, L., Lou, Q., , and Ludwig, V.: Step-by-Step Validation of Antarctic ASI AMSR-E Sea-Ice Concentrations by MODIS and an Aerial Image, IEEE TRANSACTIONS ON GEOSCIENCE AND REMOTE

360   SENSING, 59, https://doi.org/https://doi.org/10.1109/IGARSS.2018.8518219, 2021.

Spreen, G., Kaleschke, L., and Heygster, G.: Sea ice remote sensing using AMSR-E 89-GHz channels, Journal of Geophysical Research: Oceans, 113, https://doi.org/https://doi.org/10.1029/2005JC003384, 2008.

Tian-Kunze, X., Kaleschke, L., Maaß, N., Mäkynen, M., Serra, N., Drusch, M., and Krumpen, T.: SMOS-derived thin sea ice thickness: Algorithm baseline, product specifications and initial verification, Cryosphere, 8, 997–1018, https://doi.org/10.5194/tc-8-997-2014, 2014.

365 Zine, S., Boutin, J., Font, J., Reul, N., Waldteufel, P., Gabarro, C., Tenerelli, J., Petitcolin, F., Vergely, J.-L., Talone, M., and Delwart, S.: Overview of the SMOS Sea Surface Salinity Prototype Processor, IEEE Transactions on Geoscience and Remote Sensing, 46, 621–645, https://doi.org/10.1109/TGRS.2008.915543, 2008.